

Assessment of Future Climate Change Scenario in Halaba District, Southern Ethiopia

Tesemash Abebe¹, Leta Bekele², Misrak Tamire Hessebo³

¹Department of Climate Science, Ethiopian Environment and Forest Research Institute, Addis Ababa, Ethiopia

²Department of Meteorological Data and Climatology, Ethiopia Meteorology Institute, Addis Ababa, Ethiopia

³Department of Geography and Environmental Studies, Dilla University, Dilla, Ethiopia

Email: tese.leta@gmail.com, Letaabraham@gmail.com, misraktamirehesebo@gmail.com

How to cite this paper: Abebe, T., Bekele, L. and Hessebo, M.T. (2022) Assessment of Future Climate Change Scenario in Halaba District, Southern Ethiopia. *Atmospheric and Climate Sciences*, 12, 283-296.
<https://doi.org/10.4236/acs.2022.122018>

Received: December 20, 2021

Accepted: January 26, 2022

Published: March 18, 2022

Copyright © 2022 by author(s) and Scientific Research Publishing Inc.

This work is licensed under the Creative Commons Attribution International License (CC BY 4.0).

<http://creativecommons.org/licenses/by/4.0/>



Open Access

Abstract

Climate change is one environmental threat that poses great challenges to the future development prospects of Ethiopia. The study used the statistically downscaled daily data in 30-years intervals from the second generation of the Earth System Model (CanESM2) under two Representative Concentration Pathways (RCPs): RCP 4.5 and RCP 8.5 for three future time slices; near-term (2010-2039), mid-century (2040-2069) and end-century (2071-2099) were generated. The observed data of maximum and minimum temperature and precipitation are a good simulation with the modeled data during the calibration and validation periods using the correlation coefficient (R^2), the Nash-Sutcliffe efficiency (NSE), and the Root Mean Square Error (RMSE). The projected annual minimum and maximum temperatures are expected to increase by 0.091°C, 0.517°C, and 0.73°C and 0.072°C, 0.245°C, and 0.358°C in the 2020s, 2050s, and 2080s under the intermediate scenario, respectively. Under RCP8.5, the annual minimum and maximum temperatures are expected to increase by 0.192°C, 0.409°C, and 0.708°C, 0.402°C, 4.352°C, and 8.750°C in the 2020s, 2050s, and 2080s, respectively. Besides, the precipitation is expected to increase under intermediate and high emission scenarios by 1.314%, 7.643%, and 12.239%, and 1.269%, 10.316% and 26.298% in the 2020s, 2050s, and 2080s, respectively. Temperature and precipitation are projected to increase in total amounts under all-time slices and emissions pathways. In both emission scenarios, the greatest changes in maximum temperature, minimum temperature, and precipitation are predicted by the end of the century. This implies climate smart actions in development policies and activities need to consider locally downscale expected climatic changes.

Keywords

Statistical Downscaling Model, RCP Scenarios, Climate Change

1. Introduction

The global climate is changing, and projections suggest that the rate of change will likely increase [1]. Observed changes in the Earth's climate over the past 250 years are now widely considered to have been enhanced by anthropogenic activity [2] [3]. Climate change is happening due to natural and anthropogenic activities such as the burning of fossil fuels, industrial pollution, deforestation, volcanism, forest fires, and land use changes [4].

Climate scenarios from a global climate model (GCM) are supplied on a large scale and have a scale discrepancy for climate change effects and adaptation studies that require detailed local data. The regional outputs from a GCM are therefore “downscaled” using one of two methods: dynamic downscaling or statistical downscaling, which causes trouble [5]. The Statically Downscaling Model (SDSM 4.2) was introduced by Wilby *et al.* (2002) and is a Windows-based decision support tool for the rapid development of single-site, ensemble scenarios of daily weather variables under current and future regional climate forcing [6]. It is a hybrid model based on multiple linear regressions (MLR) and the stochastic weather generator (SWG) [7]. The MLR represents the statistical empirical relevancy between NCEP large-scale climate variables (predictors) and local scale weather data (predictands) along with the process of screening predictors and the calibration of SDSM, which results in the production of several regression parameters. It establishes statistical relationships between the output from GCM at a large scale (*i.e.*, predictors) and observed data from meteorological stations at a local scale (*i.e.*, predictands) based on multiple linear regression techniques. Statistical downscaling methodologies have several practical advantages over dynamical downscaling approaches. In situations where a low-cost, rapid assessment of highly localized climate change impacts is required, statistical downscaling (currently) represents the more promising option. The SDSM yields reliable estimates of extreme temperatures, seasonal precipitation totals, and areal and inter-site precipitation behavior [8]. The SDSM calculates statistical relationships based on multiple linear regression techniques between large-scale (the predictors) and local climate variables (the predictands). At the three future time horizons of 2010-2039 (2020s), 2040-2069 (2050s) and 2070-2099 (2080s), the emission scenarios for precipitation, maximum and minimum temperature outputs are generated [9].

Climate change is the major challenging factor in Africa. Rainfall variability is a greater challenge on the African continent, which results in variation in water availability. Greater spatial variation of precipitation (from a drop of about 25% - 50% drop and rise) has been reported in East Africa. For instance, Beck and [10] have reported a decline in water availability by the 2050s. In Ethiopia, the projected mean annual temperature is found to be in the ranges of 0.9°C - 1.1°C, 1.7°C - 2.1°C, and 2.7°C - 3.4°C by 2030, 2050, and 2080 time slices, respectively (Ethiopian National Meteorological Agency, 2007). The projected mean annual maximum and minimum temperatures show a rising trend in the southeastern

part of Ethiopia [11]. The increase in large-scale mean surface temperature by the end of the twenty-first century is estimated to be between 1.1°C to 2.6°C (RCP4.5) and 2.6°C to 4.8°C (RCP8.5) [12]. The temperatures reveal an increasing trend that tends to influence precipitation, water availability, and extremes of floods and droughts [1].

The current unpredictable conditions of the climate, such as frequent flood incidence and widespread drought, influence the country's agriculture and water resources [13]. The Halaba district is part of the main rift valley areas in Ethiopia known for their frequent drought and flood incidence. The rise in temperature and the change in precipitation affect the agricultural activities and water resources of the area. As a result, the Statistical Downscaling Model is used in this study application of a downscaling approach developed in recent years for precipitation, maximum and minimum temperature based on data from Halaba-Kulito stations for the period 1981-2018. The main aim of this study is to statistically downscale and produce future climate scenarios under different representative pathways for the future daily maximum temperature, daily minimum temperature, and precipitation for the early identification of the possible associated impacts and to set adaptation priorities in order to develop climate smart actions for development policies and activities.

2. Materials and Methods

2.1. Description of the Study Area

The Halaba district is located between 7°10'N and 7°42'N latitude and 38°00'E and 38°25'E longitude in the south-eastern part of Ethiopia (Figure 1). The total area of the district is 994.66 square kilometers, with 70% flat, 27% slope, and 3% mountainous. Altitude ranges in the area from 1554 to 2149 m.a.s.l (Ethiopia Central Statistical Agency, 2013). The area is located about 315 km south of Addis Ababa and 85 km southwest of Hawassa, the capital of the Southern Nations Nationalities and Peoples Regional State and Sidama region. The administrative center is Halaba-Kulito. According to Ethiopia's central statistics agency's population projection, the total population of Halaba district was 309,658 of which 151,545 were male and 158,113 females. Of this total figure, the rural inhabitants are 244,582 (79%) and the urban population makes up 21%.

The mean annual rainfall ranges between 544 and 1271 mm, which show large spatial variability with maximum rainfall being as large as 2.34 times the minimum rainfall. The rainfall pattern is erratic and irregular in the area. Due to the severe and heavy rains, soil erosion and flooding are very common in the low-lying areas of the study area. The mean monthly minimum and maximum temperatures are 12.8°C and 26.8°C. The district is considered a “*woina degas*”, or temperate zone, having two major seasons, namely *Belg* (February, March, April, and May) and *Kiremt* (June, July, August, and September), and irrigation is practiced in some parts around the *Bilate* river. The livelihood strategy of the rural people of the area is predominantly mixed agriculture (crop production and animal husbandry).

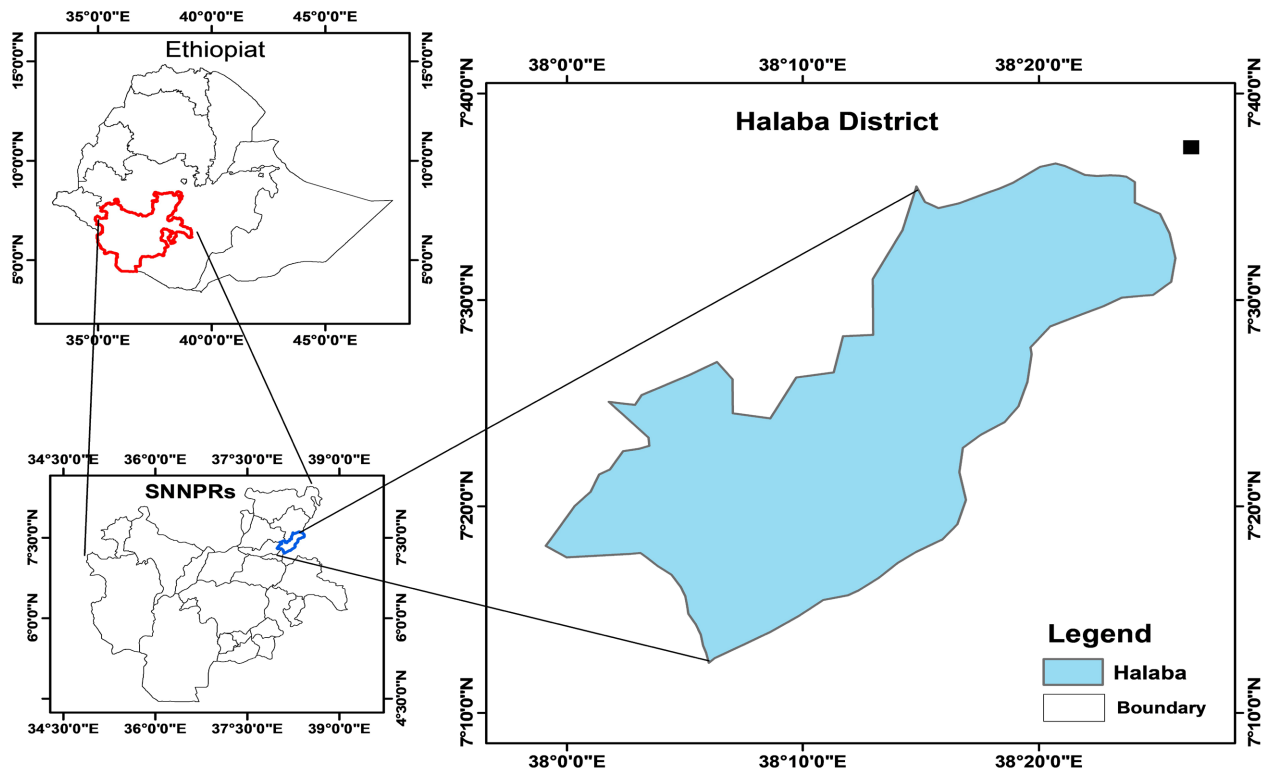


Figure 1. Map of the study area.

2.2. Data Description

The station merged grid data for rainfall and temperature for Halaba-Kulito (latitude: 7.31°S, longitude: 38.09°N) was obtained from the Ethiopian National Meteorological Agency (NMA) for the period of Jan/01/1981 to Dec/31/2018 and was used for model calibration and validation in SDSM. The baseline scenarios downscaled for base period for Halaba-kulito station using 37 years' daily data were selected to represent baseline. Thus, the CanESM2 was downscaled for the baseline period for the two RCPs scenarios and the statistical properties of the downscaled data were compared with observed data. Second Generation of Earth System Model (CanESM2): Developed at the Canadian Centre for Climate Modeling and Analysis (CCCma), this model consists of the physical coupled atmosphere-ocean model CanCM4 coupled to a terrestrial carbon model (CTEM) and an ocean carbon model (CMOC) [14]. CanESM2 provided CCCma's long-term climate simulations for Phase 5 of the Coupled Model Inter-comparison Project, which in turn informed the Fifth Assessment Report (AR5) of the Intergovernmental Panel on Climate Change [15].

2.3. Description of Statistical Downscaling Model (SDSM)

The Statistical Downscaling Model (SDSM), the well-recognized statistical downscaling tool which is applied widely in climate impact studies, was employed to transform the global circulation [16]. It is computationally inexpensive, able to directly incorporate the observational record of the region, etc. This software

manages tasks like data quality control and transformation, screening variables, model calibration, frequency analyses, statistical analysis, scenario generation, and graphing of climate data. The mathematical details of this model are provided in the study by [17]. The SDSM model contains two separate sub-models to determine the occurrence and amount of conditional meteorological variables (discrete variables), such as precipitation, and the number of unconditional variables (continuous variables), such as temperature or evaporation. Therefore, the SDSM can be classified as a conditional weather generator in which regression equations are used to estimate the parameters of daily precipitation occurrence and amount separately, making it slightly more sophisticated than a straightforward regression model [17]. The SDSM yields reliable estimates of extreme temperatures, seasonal precipitation totals, and areal and inter-site precipitation behavior. This freely available software enables the production of climate change time series at sites for which there are sufficient daily data for model calibration, as well as archived General Circulation Model (GCM) output to generate scenarios for the 21st century. The SDSM can also be used as a stochastic weather generator or to fill in gaps in meteorological data [16]. SDSM as the downscaling approach which required a proper selection of predictors established a relationship between predictors and predictand based on partial correlation coefficients. It is an important step in the downscaling process [16]. The predictors of the model were screened and selected based on the R^2 and p-values. In order to have better prediction results, all the correlations with a p-value less than 0.05 were selected (Table 1).

The delta method is a simple, widely used method to create scenario time series from GCM output. The method uses the delta method of the SDSM for future projections [5] [18]. The standard approach for the delta method is that the GCM-simulated difference for each calendar month (absolute difference for temperature and relative difference for precipitation) between a future period and the baseline period is determined and then this is superimposed on the historical daily temperature and precipitation series [19].

In the SDSM, a change in precipitation is obtained by:

$$\Delta_{2020s} = \frac{(\bar{U}_{2020s} - \bar{U}_{base}) * 100}{\bar{U}_{base}} \quad (1)$$

The same is true for changes in 2050s and 2080s.

Table 1. List of predictors chosen for each climate variable.

| Precipitation (mm) | Maximum temperature (°C) | Minimum temperature (°C) |
|-----------------------------|--------------------------------|--------------------------------|
| Surface zonal velocity | 500 hPa meridional velocity | Surface zonal velocity |
| 850 hPa wind direction | 500 hPa wind direction | 500 hPa relative humidity |
| 850 hPa geopotential height | 850 hPa airflow strength | 850 hPa meridional velocity |
| Surface-specific humidity | 850 hPa relative humidity | 850 hPa wind direction |
| | Mean temperature at 2 m height | Surface-specific humidity |
| | | Mean temperature at 2 m height |

For the absolute value calculation (temperature in this case)

$$\Delta 2020s = \bar{\vartheta}2020s - \bar{\vartheta}base \quad (2)$$

The value at 2050s and 2080s is also obtained by the same formula explained in Equation (2).

$\bar{\vartheta}$ base is the mean of all ensembles (or a specific ensemble if selected) for each statistic for the baseline period. Likewise, $\bar{\vartheta}2020s$ is the mean of all ensembles (a specific ensemble) for each statistic for period $\bar{\vartheta}2020s$, and so on for $\bar{\vartheta}2050s$ and $\bar{\vartheta}2080s$ [6].

2.4. The Representative Concentration Pathway (RCPs)

RCPs are time and space-dependent trajectories of future greenhouse gas concentrations and pollutants caused by human activities [20] [21]. It is the most recent set of time-dependent scenarios, build on this two decades development process. On the other hand, RCPs differ from earlier sets of standard situations by the radiative forcing projections, they are not emissions scenarios. The change in radiative forcing at the tropopause is connected to one value in each scenario [22] [23]. Each scenario is based on a single number: the difference in radiative forcing at the tropopause by 2100 compared to pre-industrial levels. The four RCPs are numbered 2.6, 4.5, 6.0, and 8.5 watts per square meter (W/m^2), respectively, based on the change in radiative forcing by 2100 [20] [23]. This study focuses used the RCPs 4.5 (intermediate) and 8.5 (higher) scenarios. RCP4.5 is includes the option of using policies to achieve net negative carbon dioxide emissions before the end of the century [24]. The RCP8.5 is in the absence of climate change policies, combines high population and relatively sluggish income growth with modest rates of technical advance and energy intensity gains, resulting in high long-term energy consumption and GHG emissions [20] [22].

2.5. Evaluation Criteria

Due to examining the efficiency of the proposed downscale techniques, three evaluation criteria exist: correlation coefficient, Nash-Sutcliffe efficiency, and root mean square error.

2.5.1. Correlation Coefficient

The most familiar measure of dependence between two quantities is the Pearson product-moment correlation coefficient (R^2), or “Pearson’s correlation coefficient,” commonly called simply “the correlation coefficient.” The correlation coefficient is a statistical measure of the strength of the relationship between the relative movements of your two variables. The values range between -1.0 and 1.0. A calculated number less than -1 or greater than 1 means an error in the measurement. A correlation of -1 shows a perfect correlation but is negative, while a correlation of 1 shows a perfect correlation in the positive. A correlation with 0.0 values shows no relationship between the movements of your two variables. The correlation coefficient is widely used in all categories of science.

$$R^2 = \frac{n(\sum xy) - (\sum x)(\sum y)}{\sqrt{[n\sum x^2 - (\sum x)^2][n\sum y^2 - (\sum y)^2]}} \quad (3)$$

R^2 = Correlation coefficient, n = number in the given dataset, x = first variable in the context, y = second variable.

2.5.2. Nash-Sutcliffe Efficiency

Nash-Sutcliffe efficiency (NSE) is a normalized statistic that determines the relative magnitude of the residual variance compared to the measured data variance. The Nash-Sutcliffe efficiency indicates how well the plot of observed versus simulated data fits the 1:1 line. $NSE = 1$ corresponds to a perfect match of the model to the observed data. $NSE = 0$, indicates that the model predictions are as accurate as the mean of the observed data. $Inf < NSE < 0$, indicates that the observed mean is a better predictor than the model.

$$NSE = 1 - \frac{\sum_{i=1}^n (OBS_i - SIM_i)^2}{\sum_{i=1}^n (OBS_i - \overline{OBS})^2} \quad (4)$$

OBS_i = observation value, SIM_i = forecast value, \overline{OBS} = average of observation values.

2.5.3. Root Mean Square Error

The Root Mean Square Error (RMSE) (also called the root mean square deviation, RMSD) is a frequently used measure of the difference between values predicted by a model and the values actually observed in the environment that is being modeled. These individual differences are also called residuals, and the Root Mean Square Error serves to aggregate them into a single measure of predictive power. Root Mean Square Error (RMSE) measures how much error there is between two data sets. In other words, the Root Mean Square Error compares a predicted value with an observed or known value.

$$RMSE = \sqrt{\frac{\sum_{i=1}^n (X_{obs,i} - X_{model,i})^2}{N}} \quad (5)$$

$X_{(Obs,i)}$ = observation value;

$X_{(model,i)}$ = forecast value;

N = number of the given dataset.

3. Results and Discussion

3.1. Performance of the SDSM Model Calibration and Validation

The future scenario construction, the observed data of maximum and minimum temperature and precipitation are correlated with the modeled data during the calibration and validation periods using the R^2 , NSE, and RMSE. The calibration and validation periods for Halaba-Kulito station are 1981-2002 and 2003-2018. In the unconditional process, the calibration and validation period's coefficient of determination are similar. The correlation coefficient (R^2) of determination is

0.89 for maximum temperature during calibration and validation. The minimum temperature R^2 is 0.91 during the calibration and validation period for models. The correlation coefficient of determination for precipitation is 0.85 during calibration and 0.78 during validation. The R^2 for precipitation is the lowest due to it being a conditional process and having a less regular distribution than the temperature distribution. Unconditional models assume a direct link between the regional-scale predictors and the local predictand. Conditional models, such as for daily precipitation amounts, depend on an intermediate variable such as the probability of precipitation occurrence [5]. The R^2 , NSE, and RMSE of the calibration and validation period are summarized in **Table 2**.

3.1.1. Maximum Temperature

The result of downscaling maximum temperature indicates that there is very good agreement between observed and simulated maximum temperature. During calibrated the observed and simulated data, for Halaba-Kilito climate station R^2 , NSE and RMSE to be 0.89, 0.89 and 0.36 respectively. Each regression models have a value very close to 1 for nine months. However, as shown in **Figure 2(A)**, the model overestimates the maximum temperature during the months of January, April and May. In validation process, also R^2 , NSE and RMSE model computed to be 0.89, 0.91 and 0.33 respectively. This implies, as indicated on **Figure 2(B)**, for few months (January, April and May) the model overestimates while for the other months the model showed good validation efficiency **Table 2**.

Table 2. Result of model calibration and validation.

| Station | Climate elements | Calibration | | | Validation | | |
|---------------|---------------------|-------------|------|------|------------|------|------|
| | | R^2 | NSE | RMSE | R^2 | NSE | RMSE |
| Halaba Kilito | Maximum Temperature | 0.89 | 0.89 | 0.36 | 0.89 | 0.91 | 0.33 |
| | Minimum Temperature | 0.91 | 0.81 | 0.42 | 0.91 | 0.79 | 0.46 |
| | Precipitation | 0.85 | 0.71 | 0.77 | 0.78 | 0.74 | 0.85 |

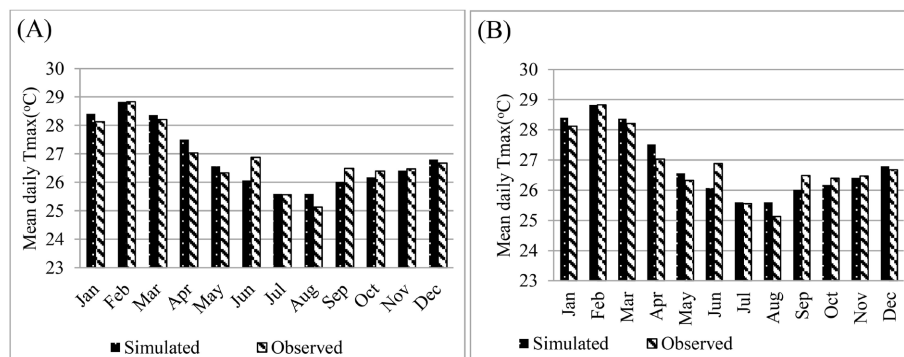


Figure 2. Calibration (A) and validation (B) results of simulated and observed mean daily maximum temperature.

3.1.2. Minimum Temperature

The result of downscaling minimum temperature indicates that there is very

good agreement between observed and simulated maximum temperature. During calibrated the observed and simulated data, for Halaba-Kilito climate station R^2 , NSE and RMSE to be 0.91, 0.81 and 0.42 respectively. Each regression models have a value very close to 1 for nine months except RMSE. However, as shown in **Figure 3(A)**, the model overestimates the minimum temperature during the months of April, November and December. In validation process, also R^2 , NSE and RMSE model computed to be 0.91, 0.79 and 0.46 respectively. This implies, as indicated on **Figure 3(B)**, during the months of February, July and December the model overestimates while for the other months of the model showed good validation efficiency **Table 2**.

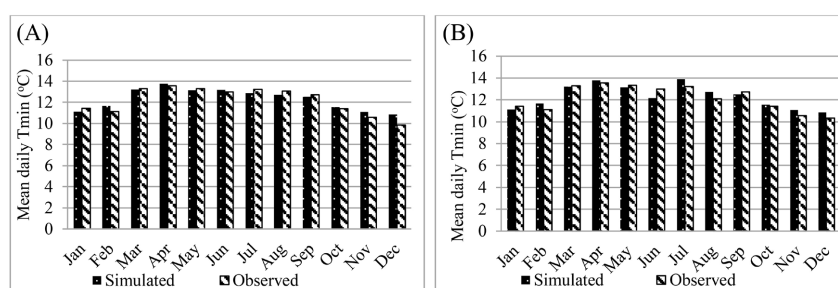


Figure 3. Calibration (A) and validation (B) results of simulated and observed mean daily minimum temperature.

3.1.3. Precipitation

Relative to the minimum and maximum temperatures, the precipitation could not be replicated to replicate the historical (observed) data. This is due to the complicated nature of precipitation processes and their distribution in space and time. Climate model simulation of precipitation has improved over time, but is still problematic. It also stated that rainfall forecasts are more uncertain than temperature forecasts. This is because rainfall is highly variable in space, and so the relatively coarse spatial resolution of the current generation of climate models is not adequate to fully capture that variability. During the calibration period observed and simulated data, for Halaba-kulito climate station R^2 , NSE and RMSE model computed to be 0.85, 0.71 and 0.77 respectively, on monthly precipitation level. While the validation period for climate station R^2 , NSE and RMSE model computed to be 0.78, 0.74 and 0.85 respectively (**Table 1 & Figure 4**).

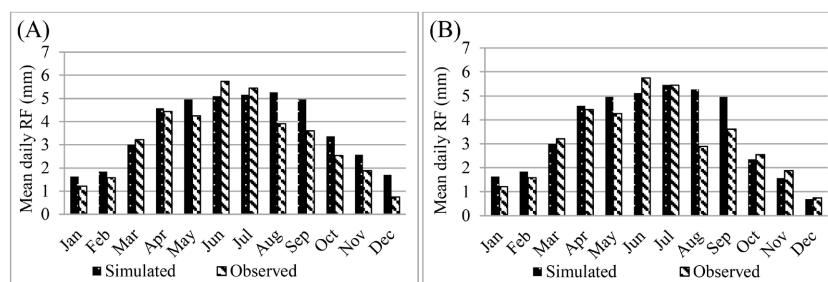


Figure 4. Calibration (A) and validation (B) results of simulated and observed mean daily precipitation.

3.2. Future Maximum and Minimum Temperature Change Scenarios

The generated future scenarios of average annual minimum and maximum temperatures generally showed an increasing trend from the base period values. The average annual minimum temperature will increase by 0.091 °C in the 2020s, 0.52 °C in the 2050s and 0.74 °C in the 2080s using RCP 4.5. In the high emissions scenario RCP 8.5, the average annual minimum temperatures increase by 0.08 °C in the 2020s, 0.84 °C in the 2050s and 1.77 °C in the 2080s. The down-scaled average annual maximum temperature scenario also indicates that it will rise by 0.07 °C in the 2020s, 0.24 in the 2050s and 0.34 °C in the 2080s using the RCP 4.5. Maximum temperatures increased by 0.4 °C in the 2020s, 4.35 °C in the 2050s, and 8.75 °C in the 2080s under the high emissions scenario RCP 8.5.

In all the scenarios, the projected average annual minimum and maximum temperatures in the 2080s are the highest. For the 2080s period, the average annual maximum temperature will increase by 8.75 °C. The average annual minimum temperature in the 2080s also increased by 1.77 °C. These results agree with the study by Kenneth *et al.* (2020) [25]. The increment in minimum temperature is less than the maximum temperature in the 2080s. This results coincides with the study of Asfaw *et al.* (2017) [26] [27]. In general, the two scenarios show an increasing pattern of average annual minimum and maximum temperatures (Figure 5).

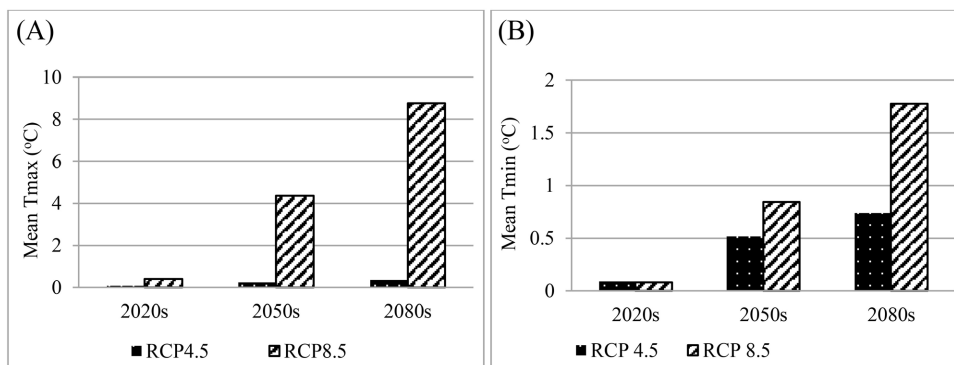


Figure 5. Projected changes in mean annual maximum temperature (A) and minimum temperature (B) in the 2020s, 2050s, and 2080s under RCP4.5 and 8.5 scenarios.

3.3. Future Precipitation Change Scenarios

The average annual precipitation will increase until the end of this century. In the model under the intermediate emissions (RCP4.5), the future average annual precipitation will be expected to increase by 1.3% in the 2020s and by 1.3% and 12.24% in the 2080s, respectively. Under the worst-case scenario RCP 8.5 scenario, the average annual precipitation is projected to increase by 1.27% in the 2020s, 10.32% in the 2050s, and 26.3% in the 2080s, respectively, compared to the baseline period.

Though the changes in the average annual precipitation value by the 2020s are not significant, as concluded from the results of future scenarios, the prediction of precipitation will increase in the 2050s and 2080s. In the 2080s, under the in-

intermediate emissions and worst-case scenarios, precipitation will increase by 12.24% and 26.3% compared to the baseline period. This results which coincides with the study of Feyissa *et al.* (2018) [5] [27]. Overall, the two scenarios show an increasing trend in the average annual precipitation (**Figure 6**).

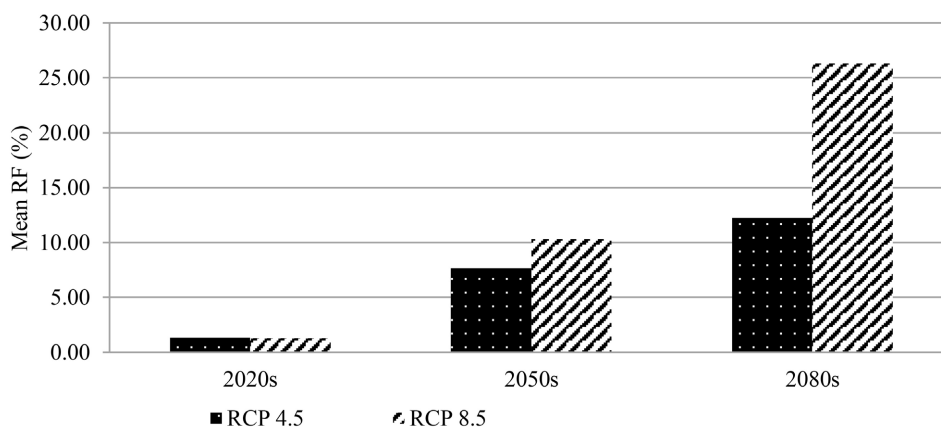


Figure 6. Projected changes in mean annual-precipitation in the 2020s, 2050s and 2080s under scenarios RCP4.5 and 8.5.

4. Conclusions

The scenarios developed for the years 2010-2099 indicate that both the minimum and maximum temperatures show an increasing trend. The predictors of the model were screened and selected based on the R^2 and p-values. During the calibration and validation periods, the SDSM model shows a good correlation between the simulated and observed results for temperature and precipitation. It also compares the results of the modeled data against the observed values for the base periods of 1981-2018 at Halaba-Kulito station. However, the results of SDSM show a slight difference between simulated and observed data for the average daily temperature and precipitation. The model results of future average annual temperature and precipitation were shown by comparing them to the baseline period (1981-2018) and three future periods (2020s, 2050s, and 2080s) under the RCP 4.5 and 8.5 scenarios.

As a result, future scenarios predict that the expected average annual temperature and precipitation will increase up to the end of the century. The changes in climatic elements up to the 2020s are not significant. However, in the 2050s and 2080s, the predictions were higher. In the worst-case scenarios, the expected average annual maximum temperature increase by 8.7°C in the 2080s. Similarly, the increase in the average annual minimum temperature reaches 1.77°C in the 2080s. All the downscaled projections under the two RCP scenarios show an increase in temperature with time, especially for RCP8.5. All the periods also predict an increase in average annual precipitation, especially in the worst-case scenarios, the volume of total average annual precipitation will also increase by 26.3% in the 2080s. Generally, the study area will experience an increase in average annual temperature and precipitation, which will gradually modify the ex-

isting temperature and precipitation conditions resulting from urbanization and climate change. The Halaba district will continue to experience drought and flooding vulnerability. Hence, it is recommended that government planning integrate the findings of this research into its planning process, which will be informative and supportive of further investigations and practical better adaptation mechanisms in the context of a climate emergency. Further studies also need to be undertaken by adding various model ensembles in order to avoid prediction inconsistency.

Acknowledgements

The authors gratefully acknowledge the Ethiopian National Meteorological Agency and the Ethiopia Environmental and Forest Research Center for providing the daily climatic data and technical support. The authors are also grateful to the developers of the SDSM tool and maintainers of the GCM-derived predictor archives for making these resources available publicly.

Authors' Contributions

Tesemash Abebe: writing the review and developed the research methodology, set up the model and tuning, and conducted the analysis; **Leta Bekele:** collected input data, helped developing the idea, supervised the analyses, and study area map production by using GIS software; **Dr Misrak Tamire Hessebo:** contributed to improving the review results and the writing process and provided critical discussions. All authors have read and agreed to the published version of the manuscript.

Conflicts of Interest

The authors declare that they have no known competing financial interests or personal relationships that could have appeared to influence the work reported in this paper.

References

- [1] Wigley, T.M.L., Jones, P.D. and Kelly, P.M. (2018) Global Warming? *Nature*, **291**, 285. <https://doi.org/10.1038/291285a0>
- [2] Angelo, M.J. and Du Plessis, A. (2017) Research Handbook on Climate Change and Agricultural Law. Research Handbooks in Climate Law Series, Edward Elgar Publishing, Cheltenham, 1-472. <https://doi.org/10.4337/9781784710644>
- [3] Venterea, R.T. (2014) Climate Change 2007: Mitigation of Climate Change. *Journal of Environmental Quality*, **38**, 837-837. <https://doi.org/10.2134/jeq2008.0024br>
- [4] Intergovernmental Panel on Climate Change (2021) Climate Change 2021: The Physical Science Basis Summary for Policymakers. Cambridge University Press, Cambridge, In Press.
- [5] Feyissa, G., Zeleke, G., Bewket, W. and Gebremariam, E. (2018) Downscaling of Future Temperature and Precipitation Extremes in Addis Ababa under Climate Change. *Climate*, **6**, Article No. 58. <https://doi.org/10.3390/cli6030058>

- [6] Wilby, R.L., Dawson, C.W. and Barrow, E.M. (2002) SDSM—A Decision Support Tool for the Assessment of Regional Climate Change Impacts. *Environmental Modelling & Software*, **17**, 145-157. [https://doi.org/10.1016/S1364-8152\(01\)00060-3](https://doi.org/10.1016/S1364-8152(01)00060-3)
- [7] Harpham, C. and Wilby, R.L. (2005) Multi-Site Downscaling of Heavy Daily Precipitation Occurrence and Amounts. *Journal of Hydrology*, **312**, 235-255. <https://doi.org/10.1016/j.jhydrol.2005.02.020>
- [8] Abbasnia, M. and Toros, H. (2016) Future Changes in Maximum Temperature Using the Statistical Downscaling Model (SDSM) at Selected Stations of Iran. *Modeling Earth Systems and Environment*, **2**, Article No. 68. <https://doi.org/10.1007/s40808-016-0112-z>
- [9] Nigatu, Z.M., Rientjes, T. and Haile, A.T. (2016) Hydrological Impact Assessment of Climate Change on Lake Tana's Water Balance, Ethiopia. *American Journal of Climate Change*, **5**, 27-37. <https://doi.org/10.4236/ajcc.2016.51005>
- [10] Niang, I., Ruppel, O.C., Abdrabo, M., Ama, E., Lennard, C., Padgham, J., *et al.* (2015) "Africa". In: Barros, V.R., Field, C.B., Dokken, D.J., Mastrandrea, M.D., Mach, K.J., Bilir, T.E., *et al.*, Eds., *Climate Change 2014: Impacts, Adaptation, and Vulnerability. Part B: Regional Aspects. Contribution of Working Group II to the Fifth Assessment Report of the Intergovernmental Panel on Climate Change*, Cambridge University Press, Cambridge, 1199-1266.
- [11] Shawul, A.A., Chakma, S. and Melesse, A.M. (2019) Regional Studies the Response of Water Balance Components to Land Cover Change Based on Hydrologic Modeling and partial least squares regression (PLSR) Analysis in the Upper Awash Basin. *Journal of Hydrology: Regional Studies*, **26**, Article ID: 100640. <https://doi.org/10.1016/j.ejrh.2019.100640>
- [12] Wongtanachai, J., Silamut, K., Day, N.P., Dondorp, A. and Chaisri, U. (2013) Effects of Antimalarial Drugs on Movement of Plasmodium Falciparum. *The Southeast Asian Journal of Tropical Medicine and Public Health*, **43**, 1-9.
- [13] Lines, G., Pancura, M. and Lander, C. (2006) Building Climate Change Scenarios of Temperature and Precipitation in Atlantic Canada Using the Statistical Downscaling Model (SDSM). *14th Symposium on Global Change and Climate Variations*, Long Beach, 14-18 January 2006, 41.
- [14] Segele, Z.T., Lamb, P.J. and Leslie, L.M. (2009) Seasonal-to-Interannual Variability of Ethiopia/Horn of Africa Monsoon. Part I: Associations of Wavelet-Filtered Large-Scale Atmospheric Circulation and Global Sea Surface Temperature. *Journal of Climate*, **22**, 3396-3421. <https://doi.org/10.1175/2008JCLI2859.1>
- [15] Taylor, K.E., Stouffer, R.J. and Meehl, G.A. (2012) An Overview of CMIP5 and the Experiment Design. *Bulletin of the American Meteorological Society*, **93**, 485-498. <https://doi.org/10.1175/BAMS-D-11-00094.1>
- [16] Fan, X., Jiang, L. and Gou, J. (2021) Statistical Downscaling and Projection of Future Temperatures across the Loess Plateau, China. *Weather and Climate Extremes*, **32**, Article ID: 100328. <https://doi.org/10.1016/j.wace.2021.100328>
- [17] Wilby, R.L., Dawson, C.W., Murphy, C., O'Connor, P. and Hawkins, E. (2014) The Statistical DownScaling Model-Decision Centric (SDSM-DC): Conceptual Basis and Applications. *Climate Research*, **61**, 259-276. <https://doi.org/10.3354/cr01254>
- [18] Schoof, J.T. (2003) Evaluation of the NCEP/NCAR Reanalysis in Terms of Synoptic Scale Phenomena: A Case Study from the Midwestern USA. *International Journal of Climatology*, **23**, 1725-1741. <https://doi.org/10.1002/joc.969>
- [19] Choi, G., Collins, D., Ren, G., Trewin, B. and Baldi, M. (2009) Changes in Means and Extreme Events of Temperature and Precipitation in the Asia-Pacific Network

- region, 1955-2007. *International Journal of Climatology*, **29**, 1906-1925. <https://doi.org/10.1002/joc.1979>
- [20] Riahi, K., Rao, S., Krey, V., Cho, C., Chirkov, V., Fischer, G., et al. (2011) RCP 8.5— A Scenario of Comparatively High Greenhouse Gas Emissions. *Climatic Change*, **109**, Article No. 33. <https://doi.org/10.1007/s10584-011-0149-y>
- [21] San José, R., Pérez, J.L., González, R.M., Pecci, J., Garzón, A. and Palacios, M. (2016) Impacts of the 4.5 and 8.5 RCP Global Climate Scenarios on Urban Meteorology and Air Quality: Application to Madrid, Antwerp, Milan, Helsinki and London. *Journal of Computational and Applied Mathematics*, **293**, 192-207. <https://doi.org/10.1016/j.cam.2015.04.024>
- [22] Thomson, A.M., Calvin, K.V., Smith, S.J., Page Kyle, G., Volke, A., Patel, P., et al. (2011) RCP4.5: A Pathway for Stabilization of Radiative forcing by 2100. *Climatic Change*, **109**, Article No. 77. <https://doi.org/10.1007/s10584-011-0151-4>
- [23] Masui, T., Matsumoto, K., Hijioka, Y., Kinoshita, T., Nozawa, T., Ishiwatari, S., et al. (2011) An Emission Pathway for Stabilization at 6 Wm⁻² Radiative Forcing. *Climatic Change*, **109**, Article No. 59. <https://doi.org/10.1007/s10584-011-0150-5>
- [24] Koudahe, K., Kayode, A.J., Samson, A.O., Adebola, A.A. and Djaman, K. (2017) Trend Analysis in Standardized Precipitation Index and Standardized Anomaly Index in the Context of Climate Change in Southern Togo. *Atmospheric and Climate Sciences*, **7**, 401-423. <https://doi.org/10.4236/acs.2017.74030>
- [25] Mwangi, K.K., Musili, A.M., Otieno, V.A. and Endris, H.S. (2020) Vulnerability of Kenya's Water Towers to Future Climate Change: An Assessment to Inform Decision Making in Watershed Management. *American Journal of Climate Change*, **9**, 317-353. <https://doi.org/10.4236/ajcc.2020.93020>
- [26] Asfaw, A., Simane, B., Hassen, A. and Bantider, A. (2018) Variability and Time Series Trend Analysis of Rainfall and Temperature in Northcentral Ethiopia: A Case Study in Woleka Sub-Basin. *Weather and Climate Extremes*, **19**, 29-41. <https://doi.org/10.1016/j.wace.2017.12.002>
- [27] Molla, M. (2020) Developing Climate Change Projections Using Different Representative Concentration Pathways of Emission Scenario: In the Case Jimma, Ethiopia. *Environmental science Journal Impact Factor*, **25**, Article ID: 556175. <https://doi.org/10.19080/IJESNR.2020.26.556175>